Study On The Pyrolysis Characteristics And Stepwise Heating Release Behavior Of Aroma Substances From Different Types Of Tobacco Leaves

Miao Liang[1], Wenqi Li[1], Jiao Li[2], Huijuan Dai[2], Yanbin Zhou[2*], Mengshu Ran[1], Guanyun Liu[1], and Junsong Zhang[1*]

[1] *College of Tobacco Science and Engineering, Zhengzhou University of Light Industry, Zhengzhou, 450001, P. R. China*
[2] *China Tobacco Hebei Industrial Co., Ltd, Shijiazhuang, 050051, P. R. China*
[*] *Corresponding author. E-mail: hbzyzyb@163.com (Yanbin Zhou), 13283712413@163.com (Junsong Zhang)*

Received: May. 08, 2026; Accepted: July. 13, 2026

To investigate the differences in thermogravimetric characteristics and heat release behavior of various tobacco leaves, flue-cured, oriental, and Cuibi No. 1 tobaccos were analyzed using thermogravimetric analysis coupled with a programmed heating platform and gas collection system. Partial least squares discriminant analysis (OPLS-DA) was employed to identify key differential substances across heating stages. The thermal weight-loss process for all samples comprised four stages, with characteristic parameters varying significantly among tobacco types. Oriental tobacco exhibited a higher weight-loss rate at stage II, while Cuibi No. 1 demonstrated a superior comprehensive pyrolysis index of 3.36×10^{-4} $(\%/\mathrm{min} \cdot {}^{\circ}\mathrm{C}^2)$. Kinetic analysis revealed that the F1.5-order chemical reaction model adequately described the decomposition processes. Activation energy at stage II ranged from 54.30 to 89.20 kJ/mol, with flue-cured tobacco showing significantly higher activation energy at stage III than the other two types. Stage II was identified as the primary phase for aroma product formation, where the total release amount followed the order: flue-cured tobacco (15,278.56 μg/g) > oriental tobacco (14,974.00 μg/g) > Cuibi No. 1 (13,190.34 μg/g), with aroma components accounting for over 84% of the total aroma compounds for each variety. OPLS-DA identified 20, 10, and 5 key differential substances for stages II, III and IV, respectively. These findings provide data support for understanding quality characteristics of tobacco materials and may offer guidance for product formulation design.

Keywords: thermogravimetric characteristics; stepwise heating; tobacco leaf type; heat released products; partial least squares discriminant analysis

http://dx.doi.org/10.6180/jase.202611_34.027

1. Introduction

Tobacco products are made by combining different tobacco leaf raw materials with tobacco materials through a rolling process. During the pyrolysis and combustion process, the tobacco raw materials undergo complex physical and chemical reactions to transform into inhalable smoke. These processes include the distillation and transfer of volatile aroma components, as well as the cracking, polymerization, and cyclization of macromolecules. Among these processes, the substances generated by the distillation pyrolysis of tobacco raw materials in an oxygen-deficient environment (200-800 °C) are crucial in influencing smoke release and sensory quality. Therefore, studying the pyrolysis characteristics and differences in heat release products of different tobacco raw materials is of great significance for understanding the smoke formation mechanism and guiding product raw material formulation.

Currently, scholars both domestically and internationally have conducted extensive research on the pyrolysis characteristics of tobacco leaves and the generation of their

heat-releasing products. For example, Siurana et al. [1] used the TG-FTIR coupled method to study the pyrolysis characteristics of tobacco and glycerol mixtures, finding that glycerol altered the composition of tobacco pyrolysis gaseous products and increased the generation of heat-releasing products at different temperatures. Wu et al. [2] identified four stages in the pyrolysis and combustion process of tobacco: water evaporation, thermal decomposition of substances such as hemicellulose/pectin, cellulose decomposition and oxidation, and lignin decomposition. They obtained the activation energies of the pyrolysis and combustion processes by thermal analysis kinetics. Liang et al. [3] studied the effects of acid washing pretreatment on the pyrolysis process of tobacco stalks, finding that acid washing altered the crystal structure of tobacco cellulose, increasing the overall pyrolysis index and reactivity of tobacco. In addition, Liang et al. [4] studied the pyrolysis and product release characteristics of cigar tobacco leaves under different glycerol gradient application rates. Their results showed that glycerol exerted the greatest impact on stage II of cigar tobacco pyrolysis, increased the pyrolysis activation energy and the content of heatreleased aroma compounds in this stage. These studies indicate that the pyrolysis characteristics and heat-released products of tobacco raw materials are influenced by the physicochemical properties of the raw materials themselves and the processing conditions.

In fact, the physicochemical properties of tobacco raw materials differ significantly among different types of tobacco, which may lead to differences in the pyrolysis characteristics and heat release products of different types of tobacco. For example, Adam et al. [5] studied the differences in pyrolysis products of three types of tobacco (Bury, Virginia and Oriental) based on pyrolysis single-photon ionization timeof-flight mass spectrometry; Zhang et al. [6] found out that there were differences in the parameters of the pyrolysis process stages of different types of tobacco raw materials, and that there was a significant correlation between the pyrolysis process parameters and the sensory quality indicators of the products. However, previous studies have predominantly focused on the overall pyrolysis behavior across the entire temperature range or on the products generated at a single pyrolysis temperature, with limited attention paid to the temperature-dependent differences in the release of aroma compounds from tobacco. In fact, the compositional changes in release products among distinct pyrolysis stages are of greater practical relevance for understanding tobacco quality and for guiding product formulation design.

This study focuses on common flue-cured tobacco, specialty flue-cured tobacco (Cuibi No. 1), and oriental tobacco. The pyrolysis characteristics of different tobacco leaves were compared by the thermogravimetric analysis (TGA) and thermal analysis kinetics methods. A programmed temperature-controlled heating platform coupled with a flue gas capture device and gas chromatography-mass spectrometry (GC-MS) was constructed to investigate the differences in heat-released aroma compounds under stepwise pyrolysis conditions. Furthermore, partial least squares (OPLS-DA) were applied to analyze the key substances that differentiated different tobacco across various heating temperature ranges. This study may provide fundamental data and references for understanding the pyrolysis characteristics of raw materials and guiding formulation design.

2. Materials and methods

2.1. Materials, Reagents and Instruments

Experimental materials: Middle leaves of flue-cured tobacco (originating from Yuxi City, Yunnan Province), middle leaves of oriental tobacco (originating from Baoshan City, Yunnan Province), and middle leaves of Cuibi No. 1 flue-cured tobacco (originating from Sanming City, Fujian Province, hereinafter referred to as Cuibi No. 1) were all provided by Hebei China Tobacco Industry Co., Ltd..

Experimental reagents: Phenylacetyl acetate (>99%, Beijing Bailingwei Technology Co., Ltd.), dichloromethane, ethanol (analytical grade, Tianjin Damao Chemical Reagent Factory).

Experimental instruments: 8890/5977A gas chromatograph-mass spectrometer (Agilent Technologies, USA), plant pulverizer (Haomai Electric Co., Ltd.), programmed temperature-controlled heating platform coupled with flue gas capture device (self-built in the laboratory, schematic diagram of the results is shown in Fig. 1), STA6000 thermogravimetric analyzer (Platinum Elmer, USA), Q5-5A laboratory mini shredder (Kaifeng Jielimeijia Machinery Equipment Co., Ltd.), PL203 electronic analytical balance (Mettler-Toledo).

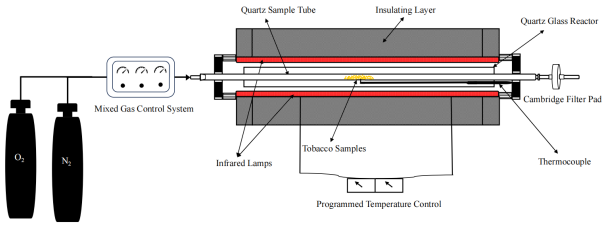

Fig. 1. Schematic diagram of programmed heating platform and gas collection system

2.2. Experimental Methods

2.2.1. Preparation of Tobacco Powder Samples

Three types of tobacco leaves were rehydrated and destemmed. The destemmed leaves were collected and uniformly shredded into 1mm wide tobacco shreds using a small laboratory shredder. The tobacco shreds were then dried in a 40 °C oven, followed by pulverizing with a plant pulverizer for 30 seconds and sieving successively. The raw materials with a particle size between 40-60 mesh were collected, dried and then stored for subsequent experiments.

2.2.2. Thermogravimetric analysis and kinetic analysis methods

20 mg of tobacco dust prepared from different types of tobacco leaves was accurately weighed and then placed into the crucible of a thermogravimetric analyzer. The thermogravimetric analysis data was recorded under nitrogen atmosphere. The experimental parameters of the thermogravimetric analysis were set as follows: flow rate of the carrier gas was 50 mL/min, the temperature was increased from 30 °C to 600 °C at a heating rate of 20 °C/min. The differential thermogravimetric curve (DTG) was obtained by the recorded and thermogravimetric curve (TG). Based on the TG-DTG curve and the tangent method, the pyrolysis stage was divided and characteristic parameters such as the maximum weight loss rate (DTG_{max}), the maximum decomposition rate temperature (T_{max}), the initial decomposition temperature (T_i), as well as the final decomposition temperature (T_f) were calculated. The comprehensive pyrolysis index (CPI) of different tobacco leaves was calculated by formula (1):

$$CPI = \frac{DTG_{\max}}{T_{\max} \times \left(T_f - T_i\right)} \tag{1}$$

Pyrolysis kinetic analysis method: The pyrolysis weight loss of tobacco leaves is a typical solid-gas heterogeneous reaction process, and its reaction rate equation can be expressed by formula (2), In the formula, α is the reaction conversion rate at time t, α = (mi - mt)/(mi - mf); mi, mt, and mf are the masses of different tobacco leaves at the beginning, intermediate time t, and end time, respectively; $f(\alpha)$ is the general expression for the reaction mechanism; k(T) is the reaction rate constant according to Arrhenius's law as following.

$$\frac{d\alpha}{dt} = k(T)f(\alpha) \tag{2}$$

$$k(T) = A\exp\left(-\frac{E_a}{RT}\right) \tag{3}$$

Wherein A and Ea represent the pre-exponential factor (min- $^{-1}$) and activation energy (kJ/mol), respectively; R is the gas constant (8.314 J/K mol), and T is the absolute temperature (K).

Combining equations (2) and (3), and given the heating rate $\beta = dT/dt$, we can simplify it to obtain:

$$\frac{d\alpha}{dT} = \frac{A}{\beta}\exp\left(-\frac{E_a}{RT}\right) f(\alpha) \tag{4}$$

After separating the variables and integrating equation (4), it can be expressed as:

$$G(\alpha) = \int_0^{\alpha} \frac{d\alpha}{f(\alpha)} = \int_{T_0}^{T} \frac{A}{\beta}\exp\left(-\frac{E_a}{RT}\right) dT \tag{5}$$

Wherein $G(\alpha)$ is the integral form of the reaction model $f(\alpha)$.

The thermogravimetric analysis of different types of tobacco leaves was performed using the Coats-Redfern method, and the results can be expressed as follows after simplification:

$$\ln\left[\frac{G(\alpha)}{T^2}\right] = \ln\left[\frac{AR}{\beta E_a}\left(1 - \frac{2RT}{E_a}\right)\right] - \frac{E_a}{RT} \tag{6}$$

Since the value of 2RT/Ea is close to zero, the above equation can be simplified to:

$$\ln\left[\frac{G(\alpha)}{T^2}\right] = \ln\left(\frac{AR}{\beta E_a}\right) - \frac{E_a}{RT} \tag{7}$$

Afterwards, Ea and A during the thermogravimetric process of different types of tobacco can be calculated from the slope and intercept of the linear fit of $\ln\left[G(\alpha)/T^2\right]$ to 1/T.

In addition, the thermodynamic parameters such as enthalpy change (ΔH), Gibbs free energy change (ΔG), and entropy change (ΔS) during the thermal weight loss process can be calculated according to formulae s (8) to (10) [7]:

$$\Delta H = E_a - RT_{\max} \tag{8}$$

$$\Delta G = E_a + RT_{\max}\ln\left(\frac{K_B T_{\max}}{hA}\right) \tag{9}$$

$$\Delta S = \frac{\Delta H - \Delta G}{T_{\max}} \tag{10}$$

In the formula, K_B is Boltzmann's constant, 1.381×10^{-23} J/K; h_A is Planck's constant, 6.626×10^{-34} J · s.

2.2.3. Capture of released products under stepwise heating conditions

A self-developed programmable temperature-controlled heating platform coupled with a flue gas capture device was used to capture the stepwise pyrolysis products of tobacco leaves within different heating temperature ranges. A schematic diagram of the device is shown in Fig. 1. This

device features simple operation and convenient control of heating temperature/atmosphere. 0.4 g of tobacco dust sample was accurately weighed into a quartz boat which was placed in the infrared heating zone. Stepwise heating conditions were set for different types of tobacco leaves using a temperature control system. The corresponding stepwise heating temperature range for each sample was determined by the sample's DTG curve and shown in Fig. 2. While the thermal released products within each stepwise heating temperature range was captured by a Cambridge filter.

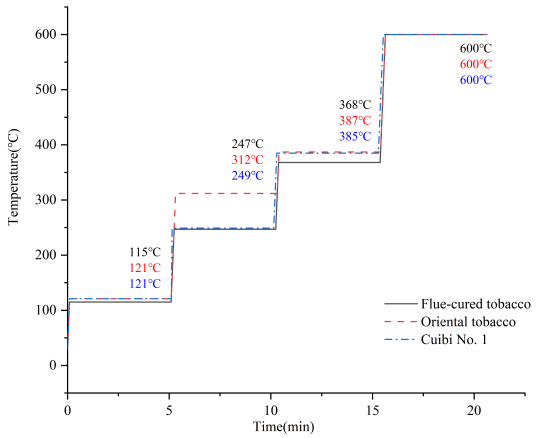

Fig. 2. Stepwise heatign procedure of different tobacco samples

The heating temperature of each stage corresponds to the termination temperature of the corresponding weight-loss stage derived from the DTG curves of each tobacco sample. The temperature is maintained at the corresponding temperature for 5 minutes to ensure complete release and collection of pyrolytic products[8]. This temperature-setting strategy, which is based on the specific thermal weight-loss stage temperatures of different tobacco, together with the relatively long holding time, provides favorable conditions for the comparison of pyrolytic products release differences among various tobacco.

2.2.4. GC/MS analysis of released products under stepwise heating conditions

Cambridge filters used to collect the pyrolysis products under each step of the heating process were transferred to 150 mL Erlenmeyer flasks. 60 mL of dichloromethane was added, after that, the mixture was ultrasonically extracted under 200 W for 30 min to obtain the pyrolysis product extract. 1 mL of the internal standard (0.2500mg/mL phenethyl acetate-dichloromethane) was added into the extract, while the volume was concentrated to 1 mL before injection for GC/MS analysis.

GC analysis conditions: Agilent HP-5 column (60 m $\times$ 250μ m $\times$ 0.25μ m), highpurity helium was used as the carrier gas; injection port temperature was 280 °C; with the carrier gas flow rate of 1.0 mL/min; split ratio of 5:1; injection volume of 1μ L; temperature program is as following: initial column temperature of 50 °C, holding for 2 min, followed by increasing to 280 °C at a rate of 8 °C/min and then holding for 25 min.

MS analysis conditions are as follows: at EI ionization mode, with ionization energy of 70 eV, transfer line temperature of 280°C, ion source temperature of 230°C, quadrupole temperature of 150 °C. While at full scan mode, the mass scan range is within 30-550 m/z. Compounds with a match factor greater than 85% against the NIST mass spectral library were considered as positively identified.

2.3. Data Processing and Analysis

The heat release products of each tobacco leaf sample were measured for three times, and the content data of each substance are expressed as average values. Thermogravimetric curves were plotted using an Origin 2021 software, while OPLS-DA analysis was performed on the volatile component data of different tobacco samples using a SIMCA 14.1 software. OPLS-DA is a supervised discriminant analysis method that achieves sample classification by maximizing inter-class differences while minimizing intra-class variations.

3. Results and discussion

3.1. Analysis of the thermogravimetric process for different tobacco leaves

Fig. 3 shows the TG and DTG curves of flue-cured tobacco, oriental tobacco, and Cuibi No. 1 tobacco leaves. The thermogravimetric curves of different tobacco leaf samples are different significantly. As can be seen from the DTG curves that, the thermogravimetric process of each tobacco leaf raw material can be divided into four stages, which correspond to the dehydration and drying stage (stage I), the volatile component release stage (stage II), the hemicellulose and cellulose decomposition stage (stage III), as well as the lignin decomposition and carbonization stage (stage IV). Among them, the temperature of stage II of the thermogravimetric process of oriental tobacco is relatively high.

Table 1 summarizes the temperature range and weight loss rate of flue-cured tobacco, oriental tobacco, and Cuibi No. 1 tobacco leaves at each weight loss stage. The temperature range and weight loss rate of different tobacco leaf samples did not differ significantly during the drying

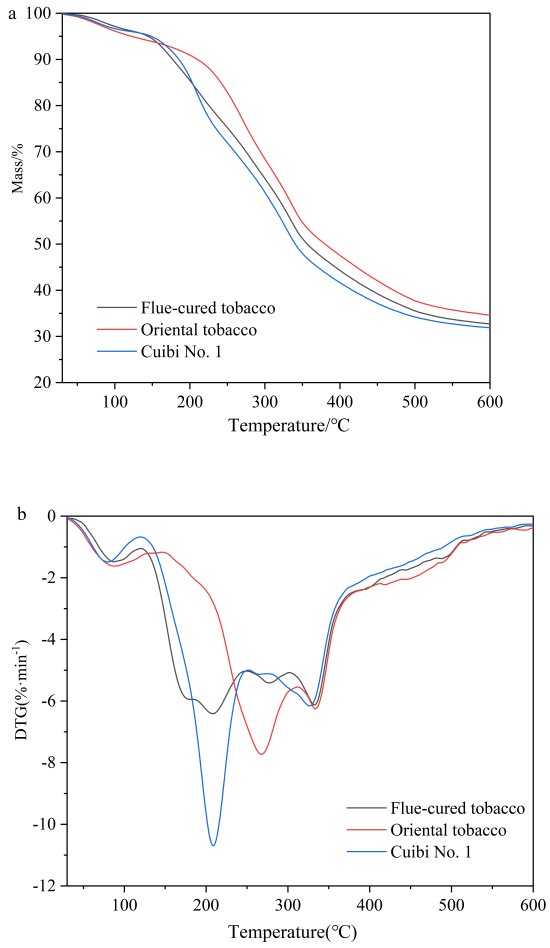

Fig. 3. TG (a) and DTG (b) curves of different types of tobacco samples

and dehydration stage. However, at stage II, where volatile components were analyzed, the weight loss rates of different tobacco leaf samples differed significantly, showing the order as follows: oriental tobacco (29.1%)> Cuibi No. 1(24.2%) > flue-cured tobacco (20.6%). This is related to the higher content of volatile aroma components in oriental tobacco and Cuibi No. 1 tobacco as compared with the flue-cured tobacco from Yunnan. The proximate analysis results as shown in Table S1 also indicated that volatile matter of oriental tobacco and Cuibi No. 1 was higher than that of flue-cured tobacco. At stage III of hemicellulose and cellulose decomposition, the overall temperature range for weight loss was $246.6 - 386.6°C$, and the weight loss rate of each sample ranged from 21.1% to 32.0%. The weight loss rate of the oriental tobacco was relatively low at stage III, which may related to the low content of cellulose components. At stage IV of thermal weight loss, the overall temperature range was between 367.7 and 600 °C. Furthermore, the weight loss rate of Cuibi No. 1 was relatively low at stage IV (11.3%).

Ti and T_f of each tobacco leaf were calculated using the TG-DTG tangent method, and the weight loss characteristics of the tobacco leaves are summarized in Table 2. The initial decomposition temperature of flue-cured tobacco was 138.4°C, lower than that of both the oriental tobacco and Cuibi No. 1, but its T_f was 435.5°C, higher than that of the oriental tobacco (394.8°C) and Cuibi No. 1 (338.0°C). At stage II, the T_{max} of different tobacco leaf samples showed the order of the oriental tobacco > Cuibi No. 1 > the flue-cured tobacco, the higher T_{max} of oriental tobacco could be attributed to its elevated contents of resins and waxy components, which possess greater thermal stability and require higher temperatures for sufficient volatilization. On the other hand, the DTG_{max} showed the order of Cuibi No. 1 > the oriental tobacco > the flue-cured tobacco. The higher DTG $_{max}$ of Cuibi No. 1 is primarily ascribed to its higher sugar content and unique chemical composition, which promote intensive Maillard reactions and release behavior during heating. The T_{max} of flue-cured tobacco at stage III (334.6°C) was higher than that of the other two types of tobacco leaves, which may be related to its higher cellulose crystallinity [9]. While the DTG_{max} of each tobacco leaf at stage III did not differ substantially. The residual pyrolysis mass of different tobacco leaves varies. Cuibi No. 1 exhibits the lowest residual pyrolysis mass (31.9%), indicating that its thermal decomposition is more complete during the entire thermal weight loss process. This was corresponded to the relatively lower content of fixed carbon. Moreover, the comprehensive pyrolysis index of Cuibi No. 1 is 3.36×10^{-4} $\left(\%/\text{min} \cdot °\text{C}^2\right)$, which is higher than that of the flue-cured tobacco and the oriental tobacco. This is attributed to the higher decomposition rate and narrower decomposition temperature of its main components.

3.2. Kinetic Analysis of Thermal Decomposition of Different Tobacco Leaves

The kinetic and thermodynamic parameters of the main pyrolysis stages II-IV of different types of tobacco leaf samples were calculated using the Coats-Redfern method, and the results are shown in Table 3. The thermal decomposition of tobacco leaf samples during various temperature ranges belongs to the F1.5 order chemical reaction kinetic model, and the overall fitting correlation coefficient R^2 is greater than 0.91. It should be noted that the F1.5 model adopted here represents an apparent kinetic description of the overall pyrolysis process, rather than a detailed mechanistic model for individual components. In the present study, the pyrolysis process of tobacco was first divided

Table 1. The temperature range and weight loss of each tobacco sample during different pyrolysis stages

Sample	Stage I		Stage II		Stage III		Stage IV	
	Temperature/ °C	Weightlessness/ %	Temperature/ °C	Weightlessness/ %	Temperature/ °C	Weightlessness/ %	Temperature/ °C	Weightlessness/ %
Flue-cured tobacco	30.0-115.3	3.5	115.3-246.6	20.6	246.6-367.7	27.5	367.7-600	14.8
Oriental tobacco	37.5-121.4	2.5	121.4-311.8	29.1	311.8-386.6	21.1	386.6-600	14.4
Cuibi No. 1	37.5-120.5	2.8	120.5-248.5	24.2	248.5-384.9	32.0	384.9-600	11.3

Table 2. The pyrolysis characteristic parameters of each tobacco sample

Sample	T_i (°C)	T_{max} (°C)		DTG_{max} (%/min)		T_f (°C)	CPI ($\% \cdot min^{-1} \cdot °C^{-2}$)	Residual mass (%)
		Stage II	Stage III	Stage II	Stage III			
Flue-cured tobacco	138.4	208.6	334.6	6.4	6.1	435.5	1.03×10^{-4}	32.9
Oriental tobacco	214.4	266.0	330.1	7.6	6.2	394.8	1.58×10^{-4}	34.5
Cuibi No. 1	170.5	209.7	325.7	11.8	6.2	338.0	3.36×10^{-4}	31.9

into distinct stages based on the TG-DTG profiles. Within each individual stage, where the reaction conditions are relatively uniform, the use of a single equivalent reaction model is considered acceptable for comparing the thermal reactivity among different tobacco.

The activation energy of all tobacco leaf samples were lowest at stage II of thermogravimetric analysis, indicating that the energy required for the volatile component release stage was relatively low. The activation energies of the three tobacco in this stage were significantly negatively correlated with the oxygen content (Table S2) of the raw materials, indicating that the oxygen content affects the ease of the reaction in stage II. Furthermore, the activation energy trends of the flue-cured and the oriental tobacco samples were basically the same across the three stages of thermogravimetric analysis, with the highest activation energy at stage III. The activation energy of the flue-cured tobacco at stage III was obviously higher than that of the oriental tobacco and Cuibi No. 1, indicating that flue-cured tobacco required the highest energy in this thermal decomposition stage. The activation energy values of Cuibi No. 1 sample at stages II and III were relatively close, indicating good continuity between the volatile component release and cellulose decomposition stages. The activation energy values of all samples at stage IV ranged from 92.78 to 104.44 kJ/mol. The pre-exponential factor A reflects the number of molecules participating in the thermal reaction per unit time. The higher A value of flue-cured tobacco at stage III indicates that a larger number of activated molecules participate in the reaction per unit time within this temperature range.

ΔH indicates the energy required per unit mass of sample participating in the corresponding thermal decomposition stage. The enthalpy change of the three types of tobacco leaves at different thermogravimetric stages ranges from 49.94 to 290.22 kJ/mol. Both the flue-cured tobacco and the oriental tobacco require the highest energy in pyrolysis stage III, while Cuibi No. 1 tobacco requires the highest energy at stage IV. ΔG reflects the change in the total energy of the system during thermal decomposition. The higher the value, the more unfavorable there is for the reaction to occur. The ΔG of the three types of tobacco raw materials increases gradually as the pyrolysis stage progresses.

3.3. Analysis of thermogravimetric behavior and pyrolysis products under stepwise heating conditions

3.3.1. Thermogravimetric behavior under stepwise heating conditions

As shown in Section 2.1, the temperature ranges for each stage of thermogravimetric analysis (TGA) differ among different types of tobacco leaves, and different thermal decomposition stages correspond to the decomposition of substances with different thermal stability within the tobacco leaves. To investigate the TGA behavior of different tobacco leaf samples under stepwise heating conditions, thermogravimetric experiments were conducted based on the temperature ranges of the four TGA stages mentioned above. Fig. 4 shows the TG and DTG curves of different tobacco leaf samples under stepwise heating conditions. The figure shows that the mass loss rate is close to 0 at the end of each heating stage, indicating that the decomposition reaction and release of the corresponding components at each stage in different tobacco leaf samples are relatively complete [10].

Table 3. The pyrolysis kinetics fitting results of each tobacco sample

Sample	pyrolysis stage	Reaction Model	Fitting equation	R^2	E (kJ/mol)	A (min^{-1})	ΔH (kJ/mol)	ΔG (kJ/mol)	ΔS kJ/(mol · K)
Flue-cured tobacco	II	F1.5	$y = -8937.94x + 6.41$	0.9617	74.31	1.09×10^{8}	69.96	102.17	-6.15×10^{-2}
	III	F1.5	$y = -35430.60x + 51.57$	0.9616	294.57	1.77×10^{28}	290.22	119.78	3.25×10^{-1}
	IV	F1.5	$y = -11159.02x + 2.13$	0.9399	92.78	1.88×10^{6}	88.42	138.31	-9.52×10^{-2}
Oriental tobacco	II	F1.5	$y = -6530.81x - 0.25$	0.9489	54.30	1.02×10^{5}	49.94	112.55	-1.20×10^{-1}
	III	F1.5	$y = -15370.46x + 11.28$	0.9133	127.79	2.44×10^{10}	123.44	132.09	-1.65×10^{-2}
	IV	F1.5	$y = -12562.45x + 3.68$	0.9351	104.44	9.98×10^{6}	100.09	142.72	-8.14×10^{-2}
Cuibi No. 1	II	F1.5	$y = -10728.89x + 5.96$	0.9774	89.20	8.33×10^{7}	84.85	118.23	-6.37×10^{-2}
	III	F1.5	$y = -10808.28x + 5.22$	0.9528	89.86	4.00×10^{7}	85.51	122.09	-6.98×10^{-2}
	IV	F1.5	$y = -12057.80x + 3.13$	0.9322	100.25	5.56×10^{4}	95.89	141.07	-8.62×10^{-2}

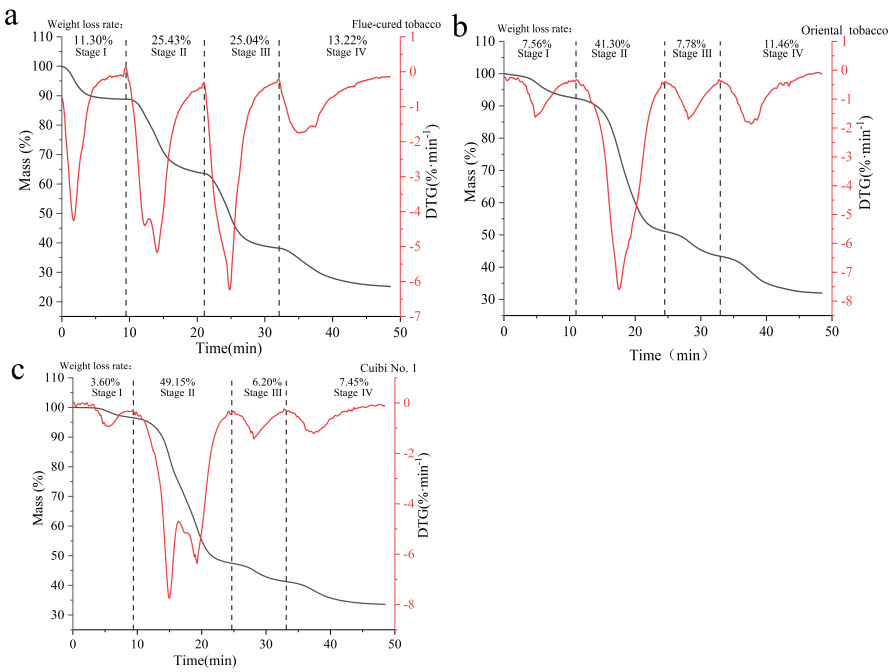

Fig. 4. TG and DTG curves of different types of tobacco samples under stepwise heating conditions (a)Flue-cured tobacco (b) Oriental tobacco (c) Cuibi No. 1

Furthermore, both the oriental tobacco and Cuibi No. 1 exhibited the highest weight loss rate at stage II of pyrolysis, on the other hand, the flue-cured tobacco showed the greatest weight loss rate at stage III. It's owing to the content of substances with different thermal stability within different tobacco leaves. The weight loss rates at different stages were calculated for each tobacco leaf. At stage II, the weight loss rate was as follows: Cuibi No. 1 (49.15%) > Oriental tobacco (41.30%) > Flue-cured tobacco (25.43%), indicating that Cuibi No. 1 tobacco leaves contain a relatively rich amount of volatile components. Additionally, the weight loss rate of the flue-cured tobacco at stage III (25.04%) and stage IV (13.22%) was higher than that of the oriental tobacco and Cuibi No. 1 tobacco leaves, suggesting differences in the content and composition of components with different thermal stability within the tobacco leaves.

3.3.2. Analysis of heat release products under stepwise heating conditions

The heat release products of each tobacco leaf under stepwise pyrolysis conditions were captured through a self-built programmable temperature-controlled heating platform coupled with a flue gas capture device. The ion chromatograms of the heat release products of different tobacco leaf samples at stages I to IV are shown in Fig. 5.

The mass loss rate of the three tobacco leaf samples at stage I was 3.6-11.3%. Although this was mainly due to the removal of moisture from the tobacco leaves, additionally, a small amount of volatile aroma components were also

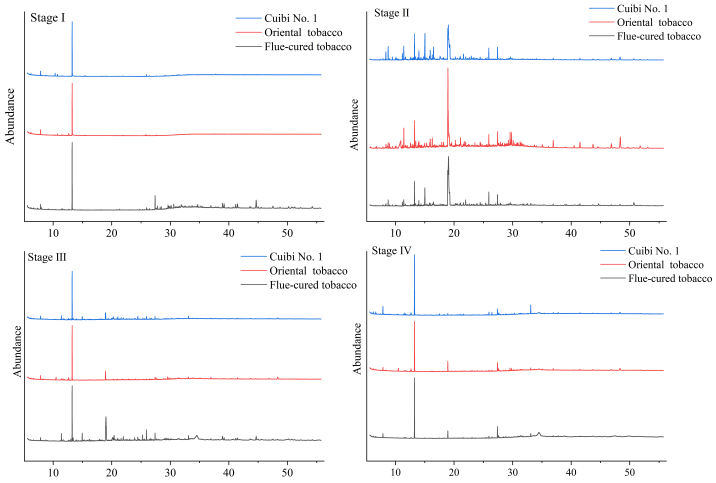

Fig. 5. Total ion chromatograms of the heating released products from flue-cured tobacco, oriental tobacco, and Cuibi No. 1 at different heating stages

detected in the heat release products of this stage. Ethyl palmitate was detected in the volatile aroma substances of all tobacco leaves. Moreover, the release amount of the flue-cured tobacco was relatively high (42.08 μg/g), which was higher than that of both the oriental tobacco and Cuibi No. 1 tobacco.

Stage II is the main stage for the formation of different heat-released products. The components quantity and contents of heat-released products in all tobacco samples increased substantially during this stage, but there were certain differences among different types of tobacco (as shown in Table 4). Some of the heat-released products in this stage derived from the distillation and transfer of the intrinsic components of the tobacco raw materials, while others came from the decomposition of polysaccharides and other components within the tobacco leaves. Nicotine was the main heat-released component in this stage for all samples. The nicotine release amount of the flue-cured tobacco was 9508.82μ g/g, higher than that of the oriental tobacco (3220.34μ g/g) and Cuibi No. 1 tobacco (5641.83μ g/g). Other alkaloids, such as nornicotine, , dienicotine, and 2,3′-bipyridine were also detected. Free neophytadiene can be directly transferred into the smoke through evaporation. The release amount of neophytadiene within different tobacco samples ranged from 280.76 to 387.34μ g/g, showing the order as the oriental tobacco > the flue-cured tobacco > Cuibi No. 1.

The heat release products also contained abundant aldehydes, alcohols, ketones, phenols, N-containing heterocyclic compounds, esters, and acids. Among them, 2-methylbutyric acid and 3-methylvaleric acid, as characteristic acids of oriental tobacco, were released in higher amounts than that of the flue-cured tobacco and Cuibi No. 1 tobacco. 2-methylbutyric acid has a cheese-like sour aroma, while 3-methylvaleric acid exhibits a sour, fruity and cheese aroma. This is closely related to the formation of the unique sour aroma style of oriental tobacco. In addition, the release of organic acids such as myristic acid and palmitic acid in the oriental tobacco is significantly higher than that in the other two types of tobacco. Furans such as furfural and furfuryl alcohol, as well as 2,3-dihydro-3,5-dihydroxy-6-methyl-4H-pyran-4-one (DDMP), are present in high contents in the thermal release products of Cuibi No. 1 tobacco. DDMP and furans have a caramel sweet aroma which are the reaction products from sugars during the heating process, indicating that the sugars in Cuibi No. 1 have a strong ability to generate caramel sweet aroma substances through the Maillard reaction due to its higher sugar content. The contents of esters such as dihydroactinol, methyl palmitate, and perillyl lactone also exhibit high content in the thermal release products of oriental tobacco. The total release of heat-released products at stage II for different tobacco was in the order of oriental tobacco (15278.56μ g/g) > flue-cured tobacco (14974.00μ g/g) > Cuibi No. 1 (13190.34μ g/g), accounting for 84.65%, 94.87%, and 93.94% of the total release of aroma substances in each tobacco leaf, respectively. The total release of aroma substances other than

Table 4. Components and amounts of heat-released products at stage II

Type	Thermal release products	Release amount/ (μg/g)		
		flue-cured tobacco	oriental tobacco	Cuibi No. 1
Hetero cyclic	2-Methylpyridine	-	23.72	-
	3,5-Dimethylpyridine	-	34.55	-
	3-Ethenyl-pyridine	-	51.87	-
	Nicotine	9508.82	3220.34	5641.83
	1-Demethyl-nicotine	168.09	148.52	-
	Nornicotine	-	115.87	33.62
	Nicotyrine	132.37	530.97	97.69
	2,3′-Dipyridyl	215.31	332.95	150.28
Furans	Furfural	98.34	224.97	274.91
	2-Furanmethanol	191.11	161.79	387.03
	1-(2-Furanyl)-ethanone	20.98	51.67	37.73
	5-Methyl-2-furancarboxaldehyde	121.23	96.68	180.82
	5-Hydroxymethylfurfural	231.13	165.93	510.63
Organic acids	2-Methylbutyric acid	-	215.62	-
	3-Methylpentanoic acid	-	1199.43	55.24
	Benzoic acid	-	-	87.85
	Benzeneacetic acid	45.78	-	41.46
	Tetradecanoic acid	49.49	217.96	35.90
	n-Hexadecanoic acid	371.59	611.70	419.81
	9,12,15-Octadecatrienoic acid	126.40	-	96.28
	Octadecanoic acid	62.88	249.39	66.2
Ketones	4-Cyclopentene-1,3-dione	49.39	66.34	98.61
	2-Methyl-2-cyclopenten-1-one	17.14	47.20	24.92
	3-Methyl-2-cyclopenten-1-one	-	57.59	32.81
	3-Methyl-1,2-cyclopentanedione	59.99	196.03	-
	2,3-Dimethyl-2-cyclopentenone	62.69	132.78	82.26
	2,5-Dimethylfuran-3,4(2H,5H)-dione	98.62	-	40.33
	3-Ethyl-2-hydroxy-2-cyclopenten-1-one	36.80	132.45	35.40
	2,3-Dihydro-3,5-dihydroxy-6-methyl-4H-pyran-4-one	768.35	273.18	1195.43
	1-(4-Methylphenyl)-ethanone	125.47	234.62	129.47
	Megastigmatrienone	126.27	244.75	214.66
	3-Hydroxy-.beta.-damascone	48.50	123.10	65.64
	9-Hydroxy-4,7-hexadecadien-3-one	36.25	288.38	75.04
	4-(2,6,6-Trimethyl-1-cyclohexen-1-yl)-2-butanone	21.96	-	-
	Cotinine	55.58	179.77	40.34
Phenols	Phenol	286.44	655.73	393.57
	2-Methyl-phenol	-	130.94	90.74
	p-Cresol	173.66	489.10	147.26
	Guaiacol	54.13	158.80	82.84
	2,5-Dimethylphenol	-	-	21.49
	Maltol	99.99	148.1	109.92
	5-Hydroxymaltol	96.95	144.03	118.61
	4-Ethylphenol		68.04	-
	2-Ethylphenol	69.23	183.73	91.16
	2,6-Dimethylphenol	-	-	11.32
	Catechol	241.11	384.23	436.16
	2-Isopropoxyphenol	64.61	159.95	114.48
	Hydroquinone	109.70	396.47	472.48
	2,6-Dimethoxyphenol	55.10	134.66	72.13
	o-Hydroxybiphenyl	76.51	-	55.73
Esters	Butyrolactone	49.58	82.36	94.92
	3-Hydroxy-gamma-butyrolactone	42.96	92.85	46.29
	Methacrylic acid, ethyl ester	147.21	120.90	190.37
	Dihydroactinidiolide	-	135.37	35.47
	Hexadecanoic acid, methyl ester	-	100.63	22.33
	Sclareolide	62.07	735.67	46.91
Alcohols	D-Limonene	36.17	84.87	-
	Pentadecene	38.83	143.38	55.30
	Longifolene	11.58	329.99	15.23
	Neophytadiene	366.38	387.34	280.76
Alcohols	Trans-geranylgeraniol	28.87	92.54	32.68
	Thunbergol	12.39	288.76	-
	Total release	14974.00	15278.56	13190.34

alkaloids such as nicotine was in the order of the oriental tobacco (11262.86μ g/g) > Cuibi No. 1(7417.20μ g/g) > the flue-cured tobacco (5164.72μ g/g).

Table 5 shows the types and contents of heat-released products for each tobacco at stage III, which were lower than that at stage II. The total amount of heat-released products from different tobacco leaves followed the order as: flue-cured tobacco (2211.26μ g/g) > Cuibi No. 1(388.94μ g/g) > oriental tobacco (769.02μ g/g). The flue-cured tobacco possessed a higher nicotine release (1248.39μ g/g), higher than that of both the oriental tobacco (111.85μ g/g) and Cuibi No. 1 (114.36μ g/g), which can be possibly ascribed to the difference in the total nicotine content and binding state in different tobacco leaves. In addition, the content of simple phenolic substances such as phenol, o-cresol, and p-cresol was relatively high in the flue-cured tobacco leaves. These phenolic substances are mostly produced from the decomposition and of polymerization cellulose and lignin, which is consistent with the higher weight loss at stage III of the stepwise thermogravimetric analysis of flue-cured tobacco. The stagespecific release behavior of eugenol, which distinguishes Cuibi No. 1 and oriental tobacco from flue-cured tobacco, may contribute to the spicy aroma profile.

Table 6 shows the contents of released components at stage IV, which exhibited an obvious decreased trend at this stage. This may be owing to the fact that the temperature was higher in this stage, and the pyrolysis products included a large amount of gases such as CO and CO_2, leading to a reduction in the captured particulate products. This phenomenon was consistent with previous studies, which indicated that the released aroma components would decrease when the pyrolysis temperature increased to 600 °C. The released contents followed the order as oriental tobacco (294.95μ g/g) > flue-cured tobacco (428.17μ g/g) > Cuibi No. 1 (76.23μ g/g). The heat released products of oriental tobacco include variety of substances in greater quantities, such as eugenol, 3-methylvaleric acid and palmitic acid. While flue-cured tobacco leaves possessed relatively higher contents of nicotine and palmitic acid in their heat-released products.

Furthermore, orthogonal partial least squares-discriminant analysis (OPLS-DA) was conducted to study the differences in released aroma component among the three types of tobacco at stage II-IV, and the result was shown in Fig. 6. In OPLS-DA, the predictive component (x-axis) captures the systematic variation related to sample class differences, while the orthogonal component (y-axis) absorbs the variation within each class that is unrelated to the classification [11, 12]. The clear spatial segregation of fluecured tobacco, oriental tobacco, and Cuibi No. 1 along the predictive axis (as shown in Fig. 6a) indicates that the volatile profiles of the three tobacco types are chemically distinct during different heating stage.

For each pyrolysis stage (II-IV), the model fit indices (Rx^2, Ry^2) and predictive ability index (Q^2) were $(0.962, 0.999, 0.998)$, $(0.967, 0.999, 0.997)$ and $(0.972, 0.991, 0.986)$, respectively, indicating an excellent model fitting result and acceptable predictive ability. To rule out the possibility of model overfitting, the fitted model was validated after 200 permutation tests, and the results were shown in Fig. 6b. The negative intercept of the Q^2 regression line (all below zero for Stages II-IV) confirmed that the models were valid and not overfitted. This result indicated that OPLS-DA model can be applied for the difference analysis of volatile components for different tobacco at stage II-IV.

Fig. 6c shows the variable importance in projection (VIP) value for different tobacco at heating stage II-IV. VIP value reflects the contribution of each variable to the classification of the model. Generally, variables with VIP > 1 are considered to play an important role in sample discrimination, and larger VIP values indicate greater contribution of the compound to distinguishing different tobacco. As shown in Fig. 6c-II, a total of 20 volatile compounds with VIP values greater than 1 were screened out, namely 4-cyclopenten-1,3-dione, nornicotine, furfural, hydroquinone, 2,6-dimethylphenol, 2,5-dimethylphenol, benzoic acid, γ-butyrolactone, furfuryl alcohol, 5-hydroxymethylfurfural, dihydro- β -ionone, 5-methylfurfural, eugenol acetate, 4,7,9-macrostigmatrien-3-one, o-cresol, DDMP, nicotine, dextrorotatory terpenes, 2,5-dimethylfuran-3,4-dione and 3-methyl-2-cyclopenten-1-one. Among them, DDMP, furfural, and 5-hydroxymethylfurfural showed elevated contents in Cuibi No. 1 tobacco, confirming its stronger Maillard reaction activity during heating. Nicotine and its derivatives were the major discriminators for flue-cured tobacco, which was consistent with its higher alkaloid content. For oriental tobacco, 2-methylbutyric acid and 3-methylvaleric acid were identified as key discriminators, reflecting its characteristic acidic aroma profile. These VIP-selected compounds thus provide both chemical and sensory interpretations for the observed differences among the three tobacco types.

Fig. 6c-III shows that a total of 10 volatile compounds with VIP values greater than 1 were screened out for heating stage III, namely nornicotine, o-phenylphenol, 2-ethylphenol, eugenol, nicotine, 3-methylvaleric acid, pyridinepyrrolidone, methyl palmitate, 2,3-dimethylphenol, and dibenzofuran. The substantially higher release of eugenol in Cuibi No. 1 and oriental to-

Table 5. Components and amounts of heat-released products at stage III

Type	Name	Release amount/ (μg/g)		
		Flue-cured tobacco	Oriental tobacco	Cuibi No. 1
Acids	3-Methylpentanoic acid	-	57.13	-
	Benzoic acid	14.54	-	-
	Hexadecanoic acid	96.92	32.97	41.65
Phenols	Phenol	106.57	16.93	66.70
	2-Methylphenol	32.29	-	16.63
	4-Methylphenol	63.25	5.10	37.06
	Guaiacol	12.45	-	6.53
	2-Ethylphenol	9.29	-	15.81
	4-Ethylphenol	18.69	-	-
	3,4-Dimethylphenol	33.58	-	16.48
	2,3-Dimethylphenol	5.72	-	4.83
	Catechol	37.35	-	11.20
	2-Ethyl-6-methylphenol	11.53	6.57	4.73
	Eugenol	-	51.78	99.41
	o-Hydroxybiphenyl	-	-	16.68
Aldehydes and ketones	2,3-Dimethyl-2-cyclopentenone	14.40	-	-
	2,3-Dihydro-3,5-dihydroxy-6-methyl-4H-pyran-4-one	125.56	-	63.01
	Cinnamaldehyde	11.86	6.73	2.26
	Megastigmatrienone	6.93	9.95	10.70
	Cotinine	22.70	5.45	7.25
	1-(2,6,6-Trimethyl-1-cyclohexen-1-yl)-1-penten-3-one	-	21.61	-
Furans	2-Methylbenzofuran	13.46	-	5.03
	Dibenzofuran	15.22	4.47	13.42
Esters	2-Methoxy-4-(2-propenyl)-phenol, acetate	48.19	5.38	39.52
	Hexadecanoic acid, methyl ester	8.17	5.87	4.80
	Sclareolide	14.54	32.02	14.63
Heterocyclic	Indole	33.42	-	-
	Nicotine	1248.39	111.85	114.36
	3-Methylindole	19.12	-	-
	3-(3,4-Dihydro-2H-pyrrol-5-yl)-pyridine	48.25	-	32.86
	Nornicotine	-	-	74.11
Alkenes	Neophytadiene	138.84	15.15	49.37
	Total release	2211.26	388.94	769.02

Table 6. Components and amounts of heat-released products at stage IV

Type	Heat release products	Release amount/ (μg/g)		
		Flue-cured tobacco	Oriental tobacco	Cuibi No. 1
Phenols	Phenol	-	-	8.82
	Eugenol	-	133.97	13.62
	Methyleugenol	7.09	8.09	1.21
Esters	2-Methoxy-4-(2-propenyl)-phenol, acetate	10.06	6.87	7.27
	Hexadecanoic acid, methyl ester	1.60	7.76	3.23
	Sclareolide	-	36.48	-
Acids	3-Methylpentanoic acid	-	65.16	-
	2,3-Dihydro-3,5-dihydroxy-6-methyl-4H-pyran-4-one	7.45	12.39	2.24
	Nicotine	140.62	132.46	39.83
Ketones	Cotinine	6.64	-	-
	Tetradecanoic acid	2.62	6.98	-
Heterocyclic	n-Hexadecanoic acid	118.85	18.01	-
	Total release	294.95	428.17	76.23

bacco suggests that these two tobacco types may exhibit more pronounced spicy aroma characteristics under heat-

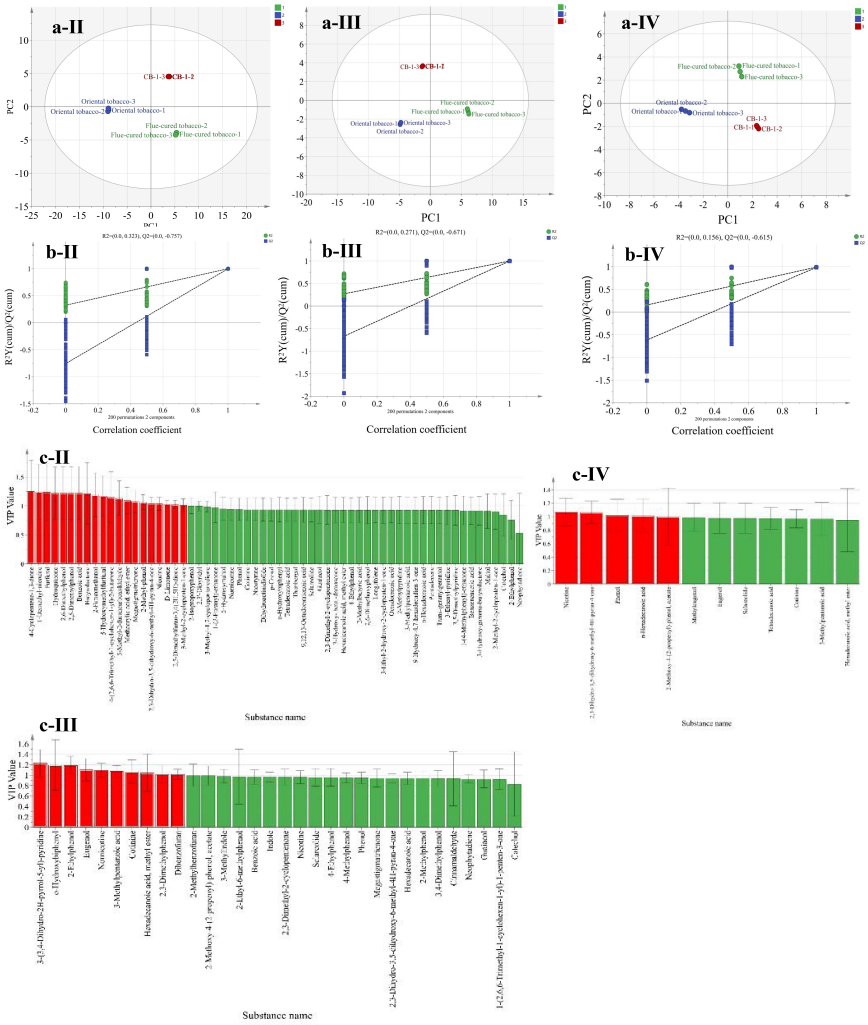

Fig. 6. OPLS-DA score diagram (a), displacement test diagram (b), and VIP value diagram (c) of volatile components in different tobacco samples at stage II-IV.

ing stage III. In contrast, the high content of 3-methylvaleric acid in oriental tobacco serves as the chemical basis for its distinctive sour and fruity aroma style. Furthermore, the marked difference in nicotine release directly accounts for the fundamental divergence in physiological strength between flue-cured tobacco and the other two tobacco types.

Fig. 6c-IV shows that five volatile components with VIP values greater than 1 were screened at stage IV, including nicotine, DDMP, phenol, palmitic acid, and eugenol acetate. The VIP-selected compounds in this stage encompass diverse chemical classes-alkaloids, Maillard reaction products, lignin-derived phenolics, fatty acids, and phenylpropanoid esters. Their differential release provides a comprehensive chemical basis for distinguishing the three tobacco types even at the high-temperature stage, where the formation of irritating and smoky notes becomes more prominent.

Fig. 7 shows the differences in the release of different substances from the three types of tobacco leaves under the whole heating conditions. It can be seen that there are certain differences in the release of aroma components among the three types of tobacco leaves. The oriental tobacco leaves release a higher content of alcohols, alkenes, esters, acids and phenols during pyrolysis. The pyrolysis components of Cuibi No. 1 tobacco leaves show a higher content of furans and aldehydes and ketones. Furans help to enhance the roasted or caramelized aroma of the smoke. Nicotine content of the flue-cured tobacco is higher, so that

heterocyclic substance content thereof is higher substantially than that of the other two types of tobacco leaves.

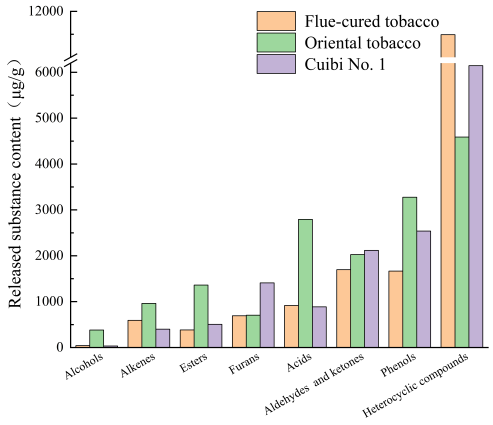

Fig. 7. Released amounts of various substances from different tobacco samples

4. Conclusion

This study comparatively investigated the pyrolysis characteristics and stepwise heat-released behavior of flue-cured tobacco, oriental tobacco, and Cuibi No. 1 using thermogravimetric analysis, kinetic modeling, and stepwise heating coupled with GC-MS analysis. The thermal weight-loss process of all three tobacco types could be divided into four stages (dehydration, volatile release, cellulose/hemicellulose decomposition, and lignin degradation/carbonization), but the temperature ranges and weight-loss rates differed notably among the samples. Oriental tobacco exhibited a higher weight-loss rate at stage II, whereas Cuibi No. 1 showed the highest comprehensive pyrolysis index, indicating superior overall thermal reactivity. Kinetic analysis indicated that an F1.5-order reaction model can described the decomposition process across stages for all samples. Stage II was identified as the dominant stage for aroma-compound formation, contributing over 84% of the total released aroma substances for each tobacco type. The total release amount at this stage followed the order: flue-cured tobacco > oriental tobacco > Cuibi No. 1. OPLS-DA further revealed that the key differential compounds varied across stages, with 20, 10, and 5 VIP-selected substances for stages II, III, and IV, respectively. Overall, the stage-dependent differences in pyrolysis behavior and aroma release observed among the three tobacco types underscore the importance of considering thermal decomposition stages when evaluating raw material quality.

Funding information:

This work was supported by the Research Foundation from China Tobacco Hebei Industrial Co., Ltd. (HBZY2024A113).

Conflict of Interest:The author declare no conflict of interest.

References

[1] A. Gomez-Siurana, A. Marcilla, M. Beltran, D. Berenguer, I. Martinez-Castellanos, and S. Menargues, (2013) *"TGA/FTIR study of tobacco and glycerol-tobacco mixtures"* **THERMOCHIMICA ACTA *573***: 146–157. DOI: 10.1016/j.tca.2013.09.007.

[2] W. Wu, Y. Mei, L. Zhang, R. Liu, and J. Cai, (2015) *"Kinetics and reaction chemistry of pyrolysis and combustion of tobacco waste"* **FUEL *156***: 71–80. DOI: 10.1016/j.fuel.2015.04.016.

[3] M. Liang, T. Yang, G. Zhang, K. Zhang, L. Wang, R. Li, Y. He, J. Wang, and J. Zhang, (2023) *"Effects of hydrochloric acid washing on the structure and pyrolysis characteristics of tobacco stalk"* **BIOMASS CONVERSION AND BIOREFINERY *13***(8): 6817–6830. DOI: 10.1007/s13399-021-01616-5.

[4] M. Liang, Y. Wang, S. Dai, L. Hong, R. Li, Z. Xu, J. Su, and J. Zhang, (2025) *"Effect of glycerol addition and heating rate on the thermal release behavior of cigar tobacco"* **BIOMASS CONVERSION AND BIOREFINERY *15***(4, SI): 6071–6086. DOI: 10.1007/s13399-024-05484-7.

[5] T. Adam, T. Ferge, S. Mitschke, T. Streibel, R. Baker, and R. Zimmermann, (2005) *"Discrimination of three tobacco types (Burley, Virginia and Oriental) by pyrolysis single-photon ionisation-time-of-flight mass spectrometry and advanced statistical methods"* **ANALYTICAL AND BIOANALYTICAL CHEMISTRY *381***(2): 487–499. DOI: 10.1007/s00216-004-2935-0.

[6] Z. Jiabao, W. Yiqun, L. Miao, Z. Xinchao, W. Dongchuan, and Z. Junsong, (2023) *"Low temperature pyrolysis characteristics of heated tobacco raw materials and its correlation with sensory quality"* **JOURNAL OF LIGHT INDUSTRY *38***(3): 94–101. DOI: 10.12187/2023.03.012.

[7] M. Liang, H. Pan, Y. Zhu, H. Zhu, M. Su, Y. Xie, Y. Zheng, X. Jiang, R. Li, and J. Zhang, (2023) *"Co-pyrolysis behavior of polylactic acid and biomass from heated tobacco products"* **BIOMASS CONVERSION AND BIOREFINERY**: DOI: 10.1007/s13399-023-04575-1.

[8] X. Jiang, J. Wu, L. Zhao, J. Wang, W. Xiao, Z. Chen, J. Jiang, M. Liang, J. Wang, and J. Zhang, (2025) *"Study on the Pyrolysis Behaviour of Different Types of Tobacco and Their Pyrolytic Aroma Components Distribution Under Stepwise Heating Conditions"* **FLAVOUR AND FRAGRANCE JOURNAL *40***(3): 512–527. DOI: 10.1002/ffj.3857.

[9] M. Liang, J. Zhang, B. Li, Q. Fu, Y. Hu, Z. Ren, R. Li, C. Cui, and J. Zhang, (2025) *"Comparative Study On The Pyrolysis Characteristics And Gaseous Release Behavior Of Different Reconstituted Tobacco Cut Stem In Processing"* **JOURNAL OF APPLIED SCIENCE AND ENGINEERING *29***(2): 359–368. DOI: 10.6180/jase.202602_29(2).0011.

[10] K. Aurreethum, V. Sricharoenchaikul, P. R. Kaewpengkrow, and M. Khemkhao, (2026) *"Enhancing Pyrolysis Oil From Landfill Waste Plastic With Industrial Waste Catalyst"* **JOURNAL OF APPLIED SCIENCE AND ENGINEERING *29***(4): 1003–1019. DOI: 10.6180/jase.202603_29(4).0023.

[11] B. Saha, S. Koley, M. Khwairakpam, and A. S. Kalamdhad, (2022) *"Comparative study between mono-digestion and co-digestion of terrestrial weed (Parthenium hysterophorus)"* **CLEANER ENGINEERING AND TECHNOLOGY *11***: DOI: 10.1016/j.clet.2022.100560.

[12] B. Saha, A. S. Kalamdhad, and M. Khwairakpam, (2021) *"Efficiency of electrohydrolysis pretreatment on terrestrial weed (Parthenium hysterophorus) to cut down the hydrolysis stage during the anaerobic digestion process and continuous reactor study"* **ENERGY REPORTS *7***: 3547–3555. DOI: 10.1016/j.egyr.2021.06.023.